

Title	Sensitivity of Nonrenormalizable Trajectories to the Bare Scale
Creators	Rosten, Oliver J.
Date	2007
Citation	Rosten, Oliver J. (2007) Sensitivity of Nonrenormalizable Trajectories to the Bare Scale. Journal of Physics A: Mathematical and Theoretical, 41 (7). 075406. ISSN 1751-8113
URL	https://dair.dias.ie/id/eprint/208/
DOI	DIAS-STP-07-17

Sensitivity of Nonrenormalizable Trajectories to the Bare Scale

Oliver J. Rosten

Dublin Institute for Advanced Studies, 10 Burlington Road, Dublin 4, Ireland

E-mail: orosten@stp.dias.ie

Abstract. Working in scalar field theory, we consider RG trajectories which correspond to nonrenormalizable theories, in the Wilsonian sense. An interesting question to ask of such trajectories is, given some fixed starting point in parameter space, how the effective action at the effective scale, Λ , changes as the bare scale (and hence the duration of the flow down to Λ) is changed. When the effective action satisfies Polchinski's version of the Exact Renormalization Group equation, we prove, directly from the path integral, that the dependence of the effective action on the bare scale, keeping the interaction part of the bare action fixed, is given by an equation of the same form as the Polchinski equation but with a kernel of the opposite sign. We then investigate whether similar equations exist for various generalizations of the Polchinski equation. Using nonperturbative, diagrammatic arguments we find that an action can always be constructed which satisfies the Polchinski-like equation under variation of the bare scale. For the family of flow equations in which the field is renormalized, but the blocking functional is the simplest allowed, this action is essentially identified with the effective action at $\Lambda = 0$. This does not seem to hold for more elaborate generalizations.

PACS numbers: 11.10.Gh, 11.10.Hi,

1. Introduction

The modern understanding of renormalization, due to Wilson [1], provides a beautifully intuitive picture of how to construct nonperturbatively renormalizable quantum field theories. To begin with, one considers a field theory as defined with some ultraviolet cutoff, Λ_0 , the bare scale. Next, one integrates out degrees of freedom between this scale and a lower, effective scale, Λ . As this procedure is carried out, the bare action evolves into the effective action, S_Λ . Since the action parametrizes the various interactions and their strengths at the appropriate scale, this evolution can be visualized as a flow in parameter space. Certain flows correspond, as we shall discuss, to renormalizable quantum field theories. These theories have the property that, *nonperturbatively*, one can send $\Lambda_0 \rightarrow \infty$, a.k.a. taking the continuum limit.

The tool to analyse the properties of the flow is the Exact Renormalization Group (ERG) equation [1, 2, 3], which is essentially the continuous version of Wilson's RG. The simplest continuum limits of some field theory follow from fixed points of the ERG equation. This is most readily seen after transferring to dimensionless units, by dividing every dimensionful quantity by Λ raised to the appropriate scaling dimension [4]. (This amounts to the rescaling step of a blocking procedure, the first step being the coarse-graining of modes.) Now, if the action is independent of Λ , it is independent of all scales and thus, in particular, Λ_0 . Consequently, fixed points of the ERG equation correspond to continuum limits.

Given a fixed point, it is possible to construct additional continuum limits by considering a flow out of this point along a trajectory which, infinitesimally close to the fixed point, is parametrized by the relevant and marginally relevant directions of the fixed point. From this, it directly follows [4] that at all points along the resulting 'Renormalized Trajectory' (RT) [1], the (rescaled) action can be written in self-similar form, meaning that it depends on Λ only through the aforementioned couplings and the anomalous dimension of the field. Such self-similar or 'perfect' actions [5] are renormalizable.

Despite the obvious importance of RTs, non-renormalizable trajectories are of interest also, particularly because there are non-renormalizable effective theories that are part of our description of nature. In particular, the Higgs and electromagnetic sectors of the standard model are not described by *nonperturbatively* renormalizable field theories (assuming that, as all the evidence suggests, nontrivial fixed points do not exist for these theories in $D = 4$). This is because both the ϕ^4 and electromagnetic couplings are marginally *irrelevant* and so cannot be used to construct an RT out of their associated Gaussian fixed points; in both cases, the only direction out of this fixed point is the mass direction and so the only RT yields massive, trivial theories. It is worth emphasising that this conclusion is, of course, completely compatible with the celebrated perturbative renormalizability of both these theories. Indeed, it is true that, perturbatively, the bare scale can be sent to infinity whilst holding the renormalized coupling fixed, as particularly efficiently demonstrated in Polchinski's classic paper [3]

(refined in [6]). However, the resulting perturbative series is ambiguous, as a consequence of ultraviolet renormalons (see [7] for a review of renormalons), indicating that the perturbative physics does not fully encapsulate the renormalizability or otherwise of the theory.

In this paper, we will study how, for nonrenormalizable trajectories, the effective action depends on the scale at which we fix the high energy parameters to take certain values. To this end, consider choosing some bare action (which does not correspond to either a fixed point or perfect action), and visualize this as a point in parameter space, together with a value for the bare scale, Λ_0 . We now wish to address the question as to how the effective action, S_Λ , varies as we vary Λ_0 , keeping the initial point in parameter space constant. Equivalently, we aim to describe how the effective action derived from some initial bare action depends on the duration of the flow. We will begin by supposing that the variation of the effective action with the *effective* scale satisfies Polchinski's form of the ERG. In this case we will show, directly from the path integral, that the variation of the effective action with the *bare* scale, keeping the interaction part of the bare action fixed, is given by an equation of the same form as the Polchinski equation, but with a kernel of the opposite sign.

Following this, we investigate whether similar equations exist for generalizations of the Polchinski equation. As we will discuss, these equations, whilst perfectly valid ERG equations, cannot be directly derived from the Polchinski equation by simply rescaling the field. Consequently, we seem to lose the path integral formalism as a means of usefully analysing the dependence of the effective action on the bare scale. There are, however, nonperturbative diagrammatic techniques that we can employ, and using these we will find that for any flow equation it is possible to construct an action which, when differentiated with respect to the bare scale (keeping the interaction part of the bare action fixed), obeys a Polchinski-like equation.

The challenge, though, is to interpret this action. In the case that we start with the Polchinski equation, we find that this action has as its vertices the n -point low energy effective action vertices. Thus, we are able to recover the conclusions of the direct, path integral approach, so long as we take $\Lambda = 0$. It remains an open question as to whether we can use the diagrammatic techniques to recover the full result obtained from the path integral approach i.e. that the effective action at *any* scale satisfies a Polchinski-like equation under variations of the bare scale.

For generalizations of the Polchinski equation, matters are not necessarily so simple. The simplest and most widely used generalization of the Polchinski equation corresponds to scaling the field strength renormalization, Z , out of the field and also rescaling the kernel, so as to remove an unwanted factor of Z which now appears on the right-hand side of the equation (it is this change to the kernel which means that the resulting flow equation is a cousin, rather than direct descendent of the Polchinski equation). Using this flow equation, we find that the action whose derivative with respect to the bare scale satisfies the Polchinski-like equation is essentially the low energy Wilsonian effective action. For more elaborate generalizations of the Polchinski equation, which

correspond to allowing an arbitrary blocking functional a.k.a. seed action [8, 9, 10, 11], it seems that this is no longer the case and we are unable to find a useful interpretation of the action appearing in the Polchinski-like equation, though this is not to say that this action cannot be computed, in principle, from the Wilsonian effective action.

Whilst the existence of these new flow equations, alone, is rather entertaining one must ask what use they might serve. Clearly, if the original ERG equation were exactly solvable, then they would be of no additional use. However, the ERG equation is not (in general) exactly solvable and so there are circumstances in which the new flow equation could lead to considerable reductions in computation time for certain calculations. For example, let us suppose that one were interested in computing the low energy effective action for a certain bare action with a range of bare scales, for some nonrenormalizable trajectory (we might be interested in doing this to obtain triviality bounds on low energy parameters). One way to do this would be to use the original flow equation, together with one's favourite approximation scheme, to compute the low energy effective action for each different value of Λ_0 (though if the trajectory spends a large amount of RG time near the Gaussian fixed point, it is necessary to do only a single ERG calculation, as one can use this as an input for a perturbative calculation which accurately generates the Λ_0 dependence [12]). Alternatively, one could do this computation for a single value of Λ_0 and then use the new flow equation to efficiently generate additional data points. It would also seem possible to dispense with using the original flow equation, at all, and just use the new flow equation(s), choosing a boundary condition at $\Lambda_0 = 0$ and integrating up to a range of sensible values of Λ_0 . (This boundary condition would involve what is essentially the finite part of the low energy effective action; for the Polchinski equation, where it is only the classical part of the kinetic term which diverges in the low energy limit, matters are particularly simple because the flow equation involves only interaction vertices.) Finally, the procedure of discovering these new flow equations has lead to some very interesting insights into the structure of the Polchinski equation, and its cousins.

The rest of this paper is organized as follows. In section 2, we begin by recalling the derivation of the Polchinski equation, directly from the path integral. Following this, we consider variations with respect to the bare, rather than effective scale, and easily derive a Polchinski-like equation for the derivative of the effective action with respect to the bare scale whilst keeping the bare interactions fixed. The diagrammatic form of the Polchinski equation, which is given in terms of the n -point ‘reduced’ (or interaction) vertices, $S_\Lambda^{R(n)}$, is introduced in section 3. Following this, we construct dressed vertices, $\overline{S}^{R(n)}$, which, in the case of the Polchinski equation, are invariant under the ERG flow and turn out to be the vertices of the low energy effective action. Irrespective of this, we then prove one of the key results of the paper, namely that the relationship between the dressed vertices and the Wilsonian effective action vertices can be inverted. To be precise, the $\overline{S}^{R(n)}$ correspond to all dressings of $S_\Lambda^{R(n)}$ with the $S_\Lambda^{R(m)}$, using the integrated ERG kernel—which is just an ultraviolet (UV) regularized propagator—for the internal lines. In a beautifully symmetric way, the $S_\Lambda^{R(n)}$ can be written as all dressing of $\overline{S}^{R(n)}$

with the $\overline{S}^{R(m)}$, but with the internal lines coming with the opposite sign.

Using this fact, there then follows the next key observation of the paper.

- (i) Starting from the Polchinski equation, we can construct the invariants, $\overline{S}^{R(n)}$. This gives us the form of the invariants admitted by equations of the same form as the Polchinski equation.
- (ii) By definition, the $S_{\Lambda=\Lambda_0}^{R(n)}$ are invariant under differentiation with respect to Λ_0 , if we keep the interaction part of the bare action fixed.
- (iii) The invariants with respect to Λ_0 , keeping the interaction part of the bare action fixed (i.e. the $S_{\Lambda=\Lambda_0}^{R(n)}$), can be constructed out of the $\overline{S}^{R(m)}$ in the same way as the $\overline{S}^{R(n)}$ can be constructed out of the $S_{\Lambda}^{R(m)}$, but with the internal lines coming with the opposite sign (and cutoff at the scale Λ_0 , rather than Λ).
- (iv) Therefore, the action whose vertices are the $\overline{S}^{R(n)}$, when differentiated with respect to Λ_0 whilst holding the bare parameters fixed, must satisfy an equation of the same form as the Polchinski equation, but with a kernel of the opposite sign (and cutoff at the scale Λ_0 , rather than Λ).

This flow equation is valid, whatever the flow equation satisfied by the Wilsonian effective action. In other words, whatever the flow equation we start with, we can always construct the functions $\overline{S}^{R(n)}$; it might just be that they are no longer invariant, under the flow. Irrespective of this, points (ii)–(iv) are always true. The relevance of point (i) is simply that it implies that equations of the same form as the Polchinski equation admit invariants with the same structure as the $\overline{S}^{R(n)}$. It is this which allows us to deduce (iv).

However, whether or not the new flow equations are useful is another matter. In section 4 we interpret the $\overline{S}^{R(n)}$ for general flow equations, finding that they have straightforward relationships to the low energy effective action only for the Polchinski equation and for its cousins with the simplest allowed blocking functional.

Finally, in section 5, we conclude.

2. The Polchinski Equation

In order to derive the new flow equation, we start by recalling the derivation of the Polchinski equation [3], for which we follow [13]. Working in D Euclidean dimensions, we begin by writing the partition function in the following form:

$$\mathcal{Z}[J] = \int \mathcal{D}\phi \exp \left(-\frac{1}{2} \phi \cdot \Delta_{\Lambda_0}^{-1} \cdot \phi - S_{\Lambda_0}^{\text{int}}[\phi] + J \cdot \phi \right). \quad (2.1)$$

The usual propagator, $\Delta(p)$, has been modified by a UV cutoff function, $C_{\Lambda_0}(p)$, which satisfies $C_{\Lambda_0}(0) = 1$ and $C_{\Lambda_0}(p) \rightarrow 0$ fast enough to regularize the theory, as $p \rightarrow \infty$: $\Delta_{\Lambda_0}(p) \equiv \Delta(p)C_{\Lambda_0}(p)$. We will often refer to propagators modified in this way as effective propagators. As usual, we employ the shorthand $J \cdot \phi \equiv J_x \phi_x \equiv \int d^D x J(x) \phi(x)$. Similarly, $\phi \cdot \Delta_{\Lambda_0}^{-1} \cdot \phi \equiv \phi_x (\Delta_{\Lambda_0}^{-1})_{xy} \phi_y \equiv \int d^D p / (2\pi)^D \phi(p) \Delta_{\Lambda_0}^{-1}(p) \phi(-p)$.

Note that in modern treatments of the Polchinski equation, the effective propagator is often taken to be massless. This does not necessarily mean that the theory is massless, because two-point terms generically appear in the interaction part of the action, $S^{\text{int}}[\phi]$. Later, we will find it useful to take the effective propagator to be massive.

We now introduce the effective scale, Λ , with the aim of integrating out modes between Λ_0 and Λ . To this end, we partition the modes, ϕ , into those above the effective scale, $\phi_>$, and those below, $\phi_<$. (For smooth cutoffs, as we use, the partitioning of modes is graduated, rather than sharp.) This is done by introducing two new cutoff functions. First, there is a UV cutoff for the low modes, C_{UV} . Secondly there is C_{IR} , which acts as an IR cutoff for the high modes, so long as they are below Λ_0 , after which it becomes the overall UV cutoff. These two cutoff functions must satisfy

$$C_{\text{UV}}(p, \Lambda) + C_{\text{IR}}(p, \Lambda, \Lambda_0) = C_{\Lambda_0}(p). \quad (2.2)$$

As in [13], we choose the two UV cutoff functions, $C_{\text{UV}}(p, \Lambda)$ and $C_{\text{UV}}(p, \Lambda_0)$, to be of the same form; i.e. $C_{\text{UV}}(p, \Lambda_0) \equiv C_{\Lambda_0}(p)$.

It now follows that the partition function can be straightforwardly rewritten, up to a discarded vacuum energy term, as [13]:

$$\mathcal{Z}[J] = \int \mathcal{D}\phi_< \mathcal{D}\phi_> \exp \left(-\frac{1}{2} \phi_< \cdot \Delta_{\text{UV}}^{-1} \cdot \phi_< - \frac{1}{2} \phi_> \cdot \Delta_{\text{IR}}^{-1} \cdot \phi_> - S_{\Lambda_0}^{\text{int}}[\phi_< + \phi_>] + J \cdot (\phi_< + \phi_>) \right). \quad (2.3)$$

Defining

$$\mathcal{Z}[J] = \int \mathcal{D}\phi_< \exp \left(-\frac{1}{2} \phi_< \cdot \Delta_{\text{UV}}^{-1} \cdot \phi_< \right) \mathcal{Z}_{\Lambda}[J, \phi_<], \quad (2.4)$$

we integrate only over the higher modes to yield [13]:

$$\mathcal{Z}_{\Lambda}[J, \phi_<] = \int \mathcal{D}\phi_> \exp \left(-\frac{1}{2} \phi_> \cdot \Delta_{\text{IR}}^{-1} \cdot \phi_> - S_{\Lambda_0}^{\text{int}}[\phi_< + \phi_>] + J \cdot (\phi_< + \phi_>) \right) \quad (2.5)$$

$$= \exp \left(\frac{1}{2} J \cdot \Delta_{\text{IR}} \cdot J + J \cdot \phi_< - S_{\Lambda}^{\text{int}}[\varphi] \right), \quad (2.6)$$

where $S_{\Lambda}^{\text{int}}[\varphi]$ is interpreted as the interaction part of the Wilsonian effective action [13, 4], and

$$\varphi \equiv \Delta_{\text{IR}} \cdot J + \phi_<. \quad (2.7)$$

Polchinski's equation (in its unscaled form [3]) follows from first recognizing that (2.5) depends on Λ only through Δ_{IR}^{-1} :

$$\frac{d}{d\Lambda} \mathcal{Z}_{\Lambda}[\phi_<, J] = -\frac{1}{2} \left(\frac{\delta}{\delta J} - \phi_< \right) \cdot \left(\frac{d}{d\Lambda} \Delta_{\text{IR}}^{-1} \right) \cdot \left(\frac{\delta}{\delta J} - \phi_< \right) \mathcal{Z}_{\Lambda}[\phi_<, J] \quad (2.8)$$

and then by substituting (2.6):

$$\frac{\partial}{\partial \Lambda} \Big|_{\varphi} S_{\Lambda}^{\text{int}}[\varphi] = \frac{1}{2} \frac{\delta S_{\Lambda}^{\text{int}}}{\delta \varphi} \cdot \frac{d\Delta_{\text{UV}}}{d\Lambda} \cdot \frac{\delta S_{\Lambda}^{\text{int}}}{\delta \varphi} - \frac{1}{2} \frac{\delta}{\delta \varphi} \cdot \frac{d\Delta_{\text{UV}}}{d\Lambda} \cdot \frac{\delta S_{\Lambda}^{\text{int}}}{\delta \varphi}. \quad (2.9)$$

Note that we have used (2.2), together with the independence of C_{Λ_0} on Λ , to write (2.9) in terms of the ultraviolet cutoff for the low modes. The function sandwiched between the pairs of functional derivatives is the ERG kernel. Sometimes we will multiply both sides of the equation through by Λ , in which case we refer to $\Lambda d\Delta_{UV}/d\Lambda$ as the kernel.

It will be useful for our analysis in section 4 to recast (2.9) in terms of the full Wilsonian effective action:

$$S_\Lambda[\varphi] = \frac{1}{2}\varphi \cdot \Delta_{UV}^{-1} \cdot \varphi + S_\Lambda^{\text{int}}[\varphi] = \hat{S}_\Lambda + S_\Lambda^{\text{int}}[\varphi]. \quad (2.10)$$

Defining

$$\Sigma_\Lambda \equiv S_\Lambda - 2\hat{S}_\Lambda \quad (2.11)$$

we can rewrite (2.9), up to a discarded vacuum energy term, as:

$$\frac{\partial}{\partial \Lambda} S_\Lambda[\varphi] = \frac{1}{2} \frac{\delta S_\Lambda}{\delta \varphi} \cdot \frac{d\Delta_{UV}}{d\Lambda} \cdot \frac{\delta \Sigma_\Lambda}{\delta \varphi} - \frac{1}{2} \frac{\delta}{\delta \varphi} \cdot \frac{d\Delta_{UV}}{d\Lambda} \cdot \frac{\delta \Sigma_\Lambda}{\delta \varphi}, \quad (2.12)$$

where we take it to be understood that it is φ which is held constant when differentiating the left-hand side with respect to Λ .

What we would like to do now is return to (2.5) and this time differentiate with respect to Λ_0 , whilst holding the interaction part of the bare action fixed. However, there is a subtlety involved in doing this, which pertains to the field strength renormalization. To illustrate this point, we note that we could have

$$S_{\Lambda_0}^{\text{int}}[\phi_{<} + \phi_{>}] = \frac{Z_{\Lambda_0}^{-1} - 1}{2} (\phi_{<} \cdot \Delta_{UV}^{-1} \cdot \phi_{<} + \phi_{>} \cdot \Delta_{\text{IR}}^{-1} \cdot \phi_{>}) + \dots, \quad (2.13)$$

where the ellipsis potentially includes a mass term and all other possible interactions; we denote the set of parameters characterising these terms by $\{P_{\Lambda_0}\}$. Now, life can be made simpler if we take the kinetic term to be canonically normalized at the bare scale i.e. we choose $Z_{\Lambda_0} = 1$ and suppose that the only two-point contribution in $\{P_{\Lambda_0}\}$ is the mass. It should thus be clear that, given this choice, we want to consider differentiating (2.5) with respect to Λ_0 , whilst keeping $\{P_{\Lambda_0}\}$ and φ fixed. This yields

$$\left. \frac{\partial}{\partial \Lambda_0} \right|_{\varphi, \{P_{\Lambda_0}\}} S_\Lambda^{\text{int}}[\varphi] = -\frac{1}{2} \frac{\delta S_\Lambda^{\text{int}}}{\delta \varphi} \cdot \left. \frac{\partial \Delta_{\Lambda_0}}{\partial \Lambda_0} \right|_{\{P_{\Lambda_0}\}} \cdot \frac{\delta S_\Lambda^{\text{int}}}{\delta \varphi} + \frac{1}{2} \frac{\delta}{\delta \varphi} \cdot \left. \frac{\partial \Delta_{\Lambda_0}}{\partial \Lambda_0} \right|_{\{P_{\Lambda_0}\}} \cdot \frac{\delta S_\Lambda^{\text{int}}}{\delta \varphi}. \quad (2.14)$$

Since we have chosen $\Delta_{UV}(p, \Lambda)$ and $\Delta_{\Lambda_0}(p)$ to have the same form, we observe that (2.14) has the same structure as (2.9), but with the kernels differing by a sign (and evaluated at a different scale). We explicitly indicate that Δ_{Λ_0} is differentiated with respect to Λ_0 whilst holding $\{P_{\Lambda_0}\}$ fixed since we are at liberty to include a mass term in Δ_{Λ_0} .

3. Invariants of the Polchinski Equation

In this section, we will demonstrate how the $\Lambda = 0$ case of (2.14) can be deduced by diagrammatic means. The first step is to write down the flow equation for the n -point vertices, $S_\Lambda^{\text{R}(n)}$, which are defined as follows:

$$S[\varphi] = \frac{1}{2}\varphi \cdot \Delta_{UV}^{-1} \cdot \varphi + \sum_n \frac{1}{n!} \int_{k_1, \dots, k_n} S_\Lambda^{\text{R}(n)}(k_1, \dots, k_n) \varphi(k_1) \cdots \varphi(k_n) \delta^{(D)}(k_1 + \dots + k_n). \quad (3.1)$$

In diagrammatic notation, we express the vertex coefficient functions as follows.

$$\Delta_{UV}^{-1}(k) = \text{circle with } \Delta_{UV}^{-1} \text{ inside, one leg with momentum } k \text{ pointing down} \quad (3.2a)$$

$$S_{\Lambda}^{R(n)}(k_1, \dots, k_n) = \text{circle with } S_{\Lambda}^R \text{ inside, } n \text{ legs with momenta } k_1, \dots, k_n \text{ pointing outwards} \quad (3.2b)$$

The $S_{\Lambda}^{R(n)}$, the ‘reduced vertices’ [14], can of course be identified with the vertices of the interaction part of the Wilsonian effective action. However, their interpretation will later be generalized, somewhat, and in anticipation of this, we refrain from explicitly denoting them as S_{Λ}^{int} . Dropping the subscript Λ s, for brevity, the diagrammatic flow equation for these vertices is shown in figure 1.

$$-\Lambda \frac{d}{d\Lambda} \left[\text{circle with } S^R \text{ inside} \right]^{(k_1, \dots, k_n)} = \frac{1}{2} \left[\begin{array}{c} \text{circle with } S^R \text{ inside} \\ \bullet \\ \text{circle with } S^R \text{ inside} \end{array} - \text{circle with } S^R \text{ inside and a dot on top} \right]^{(k_1, \dots, k_n)}$$

Figure 1. The diagrammatic form of the flow equation for vertices of the Wilsonian effective action.

The circle on the left-hand side of the flow equation just represents the n -point, Wilsonian effective action vertex with momentum arguments k_1, \dots, k_n . We will often drop the momentum arguments, replacing them simply by (n) , to indicate n external legs. Since all fields have been stripped off, we replace the derivative with respect to Λ at constant φ with a total derivative. On the right-hand side of the flow equation, the object $\text{---}\bullet\text{---}$ represents the kernel with the dot, as usual, denoting $-\Lambda \frac{d}{d\Lambda}$. The kernel attaches to vertex coefficient functions which can, in principle, have any number of additional legs. The rule for determining how many legs each of these vertices has—equivalently, the rule for decorating the diagrams on the right-hand side—is that the n available legs are distributed in all possible, independent ways. For much greater detail on the diagrammatics, see [9, 15].

At this point, there is an obvious objection to using the diagrammatic scheme to draw reliable nonperturbative conclusions. The diagrammatic flow equation follows from an expansion about vanishing field and it is well known that such expansions, when truncated at some point have generally poor convergence properties [16]‡. However, we will never perform any truncation; rather we will perform a series of exact manipulations and finally undo the expansion about vanishing field at the end. We tacitly assume that this procedure leads to well defined results.

‡ In some circumstances, though, the convergence is surprisingly good, up to a certain point [17].

Consider now the set of n -point diagrams, $\bar{S}^{R(n)}(k_1, \dots, k_n)$, defined as follows:

$$\bar{S}^{R(n)}(k_1, \dots, k_n) \equiv \sum_{s=0}^{\infty} \sum_{j=1}^{s+1} \Upsilon_{s,j} \left[\left[\textcircled{S^R} \right]^j \right]^{\Delta^s(k_1) \dots (k_n)} \quad (3.3)$$

with, for non-negative integers a and b , the definition

$$\Upsilon_{a,b} \equiv \frac{(-1)^{b+1}}{a!b!} \left(\frac{1}{2} \right)^a. \quad (3.4)$$

Note that, at present, we should identify Δ with Δ_{UV} , but we choose this more flexible notation so that expressions such as (3.3) still hold when we come to generalize the set-up in section 4.

We understand the notation of (3.3) as follows. The right-hand side stands for all independent, connected n -point diagrams which can be created from j reduced Wilsonian effective action vertices, s internal lines (i.e. effective propagators) and n external fields carrying momenta k_1, \dots, k_n . (It is the constraint of connectedness which restricts the sum over j .) The combinatorics for generating fully fleshed out diagrams is simple and intuitive. As an example of how it works, consider the diagram shown in figure 2 (for a comprehensive description see [18, 19]).

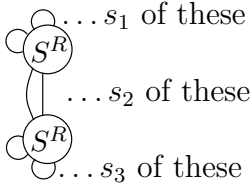


Figure 2. An example of a diagram represented by the right-hand side of (3.3), prior to decoration with the external fields.

The number of ways of generating this diagram can be worked out in two parts. First, consider the effective propagators. To create the diagram, we need to divide the s effective propagators into sets containing s_1 , s_2 and s_3 effective propagators. The rule is that the number of ways of doing this is

$${}^s C_{s_1} {}^{s-s_1} C_{s_2} {}^{s-s_1-s_2} C_{s_3} = \frac{s!}{s_1!s_2!s_3!}.$$

Next, we note that every effective propagator whose ends attach to a different vertex comes with a factor of two, representing the fact that each of these lines can attach either way round. This yields a factor of 2^{s_2} . The rule for the vertices is that they come with a factor $j!/\mathcal{S}$, where \mathcal{S} is the symmetry factor of the diagram. Thus, including the numerical factors buried in Υ , the overall factor of our example diagram is

$$\frac{1}{s_1!s_2!s_3!} \left(\frac{1}{2} \right)^{s_1+s_3} \frac{1}{\mathcal{S}}.$$

Figure 3 shows first few terms that contribute to $\bar{S}^{R(2)}$, assuming only even-point vertices exist. Decoration with the external fields gives a factor of two if they decorate different vertices, and unity if they do not.

$$\overline{S}^{R(2)} = \frac{1}{2} \text{ (circle with } S \text{ and two external lines)} - \text{ (vertical chain of two } S^R \text{ circles)} - \frac{1}{6} \text{ (vertical chain of two } S \text{ circles)} - \text{ (vertical chain of two } S \text{ circles)} + \frac{1}{8} \text{ (circle with } S \text{ and two external lines)} + \dots$$

Figure 3. The first few terms that contribute to $\overline{S}^{R(2)}$; momentum arguments are suppressed. Notice that, since reduction of the vertices only affects two-point vertices, we can remove the superscript ‘R’ from the vertices, in most cases.

To understand the interpretation of the $\overline{S}^{R(n)}$, we will compute their flow. First, though, we note that we choose to define the ERG kernel such that it includes a mass term. We do this since the expression (3.3) includes diagrams which are not one-particle irreducible (1PI) and so, with a massless ERG kernel, would develop IR divergences as the external momenta tend to zero. This, does, however, seem to be necessary only as a temporary measure, as we shall see.

Applying the diagrammatic form of the flow equation, given in figure 1, to (3.3) yields (a more complicated version of this computation is required for section 4 and is presented in Appendix A):

$$\Lambda \frac{d}{d\Lambda} \overline{S}^{R(n)}(k_i) = 0, \quad \forall n. \quad (3.5)$$

Thus we see that the $\overline{S}^{R(n)}$ are independent of Λ and so we can interpret them using any convenient value of Λ . To this end, let us choose $\Lambda = 0$: every diagram on the right-hand side of (3.3) that possesses an internal line vanishes, since

$$\lim_{\Lambda \rightarrow 0} C_{UV}(p, \Lambda) = 0. \quad (3.6)$$

This, together with (3.5), implies:

$$\overline{S}^{R(n)}(k_i) = S_{\Lambda=0}^{R(n)}(k_i), \quad (3.7)$$

which makes sense: if we consider (3.3) for $\Lambda = \Lambda_0$, then the right-hand side gives the bare n -point vertex and all of its possible dressings. This is similar to the usual Feynman diagram expansion, but where the vertices are exact, no perturbative expansion having been performed.

Remarkably enough, equation (3.3) can be inverted (we henceforth suppress momentum arguments):

$$S^{R(n)} = \sum_{s=0}^{\infty} \sum_{j=1}^{s+1} \Upsilon_{s,j} \left[\left[\overline{S}^R \right]^j \right]^{\overline{\Delta}^s(n)}, \quad (3.8)$$

where

$$\overline{\Delta} \equiv -\Delta. \quad (3.9)$$

We will prove (3.8) diagrammatically; before doing this, we briefly discuss what it tells us about the Polchinski equation. First, we note that, as emphasised already, equation (3.8)

is true irrespective of whether the $S^{R(n)}$ satisfy the Polchinski equation. However, we can consider the Polchinski equation for $V(x, t)$, with $x \in \mathbb{R}$, to be the generator of (3.3). This equation reads:

$$\dot{V} = \frac{1}{2}V'\dot{G}V' - \frac{1}{2}\dot{G}V'', \quad (3.10)$$

where $X' \equiv \partial_x X$, $\dot{X} = \partial_t X$ and $G = G(t)$. Now, this equation admits invariant with respect to t , $U(x)$. What we will prove, diagrammatically, amounts to showing that

$$U = F(V, G) \Rightarrow V = F(U, -G). \quad (3.11)$$

This can be straightforwardly shown, algebraically, in the case that we drop either of the terms on the right-hand side of (3.10).[§] Specifically, if we drop the first term in (3.10) then we have

$$V(x, t) = \exp\left(-\frac{1}{2}G(t)\frac{\partial^2}{\partial x^2}\right)U(x)$$

whereas, if we drop the second term, then the solution is defined by

$$V'(x, t) = \frac{dU(x_0)}{dx_0}, \quad x = x_0 - G(t)\frac{dU(x_0)}{dx_0}, \quad V(x, t) = U(x_0) - \frac{1}{2}G(t)\left[\frac{dU(x_0)}{dx_0}\right]^2.$$

In both cases, (3.11) is satisfied. It would be nice to extend this conclusion to solutions of the full equation, (3.10), without having to resort to the diagrammatics. That the diagrammatic solution is known may provide a clue as to how to do this, but we leave this issue open for the future.

The proof of (3.8) follows. The basic idea is to substitute (3.3) into (3.8) and collect together all terms with a *total* of j_0 vertices and s_0 effective propagators and which have the same topology. All such sets of diagrams cancel, except for the set comprising a single, undecorated vertex.

A good starting point is to consider (3.8) for $j = 1$. After substituting (3.3), it is clear that all j_0 vertices come from a single instance of \overline{S}^R , but the effective propagators come from two places. It can be intuitively helpful to think of the problem as creating a diagram out of effective propagators of two different colours.^{||} Let us suppose that $s_0 - s$ effective propagators come from the \overline{S}^R , itself. Then we can write the $j = 1$ contribution to the right-hand side of (3.8) as:

$$\Upsilon_{s_0, j_0} \sum_{s=0}^{s_0-j_0+1} (-1)^s {}^{s_0}C_s \left[\left[\left[\textcircled{S^R} \right]^{j_0} \right]^{\Delta^{s_0-s}} \right]^{\Delta^s(n)}, \quad (3.12)$$

where s cannot exceed the given upper limit due to the constraint that the parent \overline{S}^R be connected. Notice that for $j_0 = 1$ and $s_0 = 0$, we recover the left-hand side of (3.8), which is encouraging.

Were it not for the fact that the diagram has to be connected *already* after decoration with the inner effective propagators (this follows simply because \overline{S}^R contains

[§] I would like to thank Hugh Osborne for pointing this out.

^{||} I would like to thank Francis Dolan for this nice interpretation.

only connected diagrams), then we could combine inner and outer internal lines with *no change* to the combinatoric factor. (This is demonstrated as part of Appendix A). Given that we must have connectedness at the aforementioned intermediate stage, it makes sense to split up the total of s_0 effective propagators into a set of L , which link separate vertices, and a set of $s_0 - L$ which form loops on individual vertices, since the $s_0 - L$ effective propagators know nothing about connectedness. Similarly, we split s into $s - L'$ and L' , requiring that $L \geq L'$, $s_0 - s \geq L - L'$. We will sum over L' , which can run from zero to $L - j_0 + 1$, noting that the above constraints will affect the limits of the sum over s , which we will do second. Dividing up the effective propagators in this way produces the usual combinatoric factors. Since we have properly taken account of connectedness with the new limit imposed on the sum over s by the above decomposition, we can simply combine the inner and outer external lines into the two sets which we understand to either link vertices or decorate vertices:

$$\Upsilon_{s_0, j_0} s_0 C_L \sum_{L'=0}^{L-j_0+1} {}^L C_{L'} \sum_{s=L'}^{s_0-L+L'} (-1)^s {}^{s_0-L} C_{s-L'} \left[\left[\textcircled{S^R} \right]^{j_0} \right]^{\Delta_{s_0-L} \Delta^L(n)}. \quad (3.13)$$

Shifting $s \rightarrow s + L'$, it is apparent that (3.13) vanishes, unless $L = s_0$, in which case we have:

$$\Upsilon_{s_0, j_0} \delta(s_0 - L) \sum_{L'=0}^{L-j_0+1} (-1)^{L'} {}^L C_{L'} \left[\left[\textcircled{S^R} \right]^{j_0} \right]^{\Delta_{s_0}}, \quad (3.14)$$

where we understand that all effective propagators link the vertices. Thus we have proved (3.8) for the special case where $j = 1$ and where there is at least one internal line which starts and ends on the same vertex.

Let us now return to (3.8). For some value of j , say l , we will split the s effective propagators into $l + 1$ sets: s'_1, \dots, s'_l , which decorate the l \overline{S}^R s and K , which link the l \overline{S}^R s. The result is:

$$\sum_{s=0}^{\infty} \sum_{l=1}^{s+1} \Upsilon_{K,l} \delta(s - s'_1 - \dots - s'_l - K) \left[\begin{array}{c} \Upsilon_{s'_1,1} \left[\textcircled{\overline{S}^R} \right]^{\overline{\Delta}^{s'_1}} \\ \vdots \\ \Upsilon_{s'_l,1} \left[\textcircled{\overline{S}^R} \right]^{\overline{\Delta}^{s'_l}} \end{array} \right]^{\overline{\Delta}^K(n)}. \quad (3.15)$$

We immediately see that the diagrams in the big square brackets decompose into l contributions of the form (3.14), all joined together by K of the outer effective propagators. Thus, we have now proved that (3.8) works for any value of j , so long as at least one internal line starts and ends on the same vertex. Now we must prove that it works when all internal lines are links.

To this end, we suppose that the i th decorated \overline{S}^R , above, has a total of j_i vertices and s_i effective propagators. We now write down the expression for all diagrams with a

grand total of j_0 vertices and s_0 effective propagator. We have:

$$\Upsilon_{s_0, j_0} \sum_{l=1}^{j_0} \frac{j_0! s_0!}{l!} \left(\prod_{i=1}^l \sum_{j_i=1}^{j_0} \frac{1}{j_i!} \sum_{L_i=j_i-1}^{s_0-l+1} \frac{1}{L_i!} \sum_{L'_i=0}^{L_i-j_i+1} (-1)^{L'_i} {}^{L_i} C_{L'_i} \right) \delta \left(j_0 - \sum_{r=1}^l j_r \right) \sum_{K=l-1}^{s_0} \frac{(-1)^K}{K!} \delta \left(s_0 - \sum_{t=1}^l L_t - K \right) \left[\begin{array}{c} \left[\left[\textcircled{S^R} \right]^{j_1} \right]^{\Delta_{L_1}} \\ \vdots \\ \left[\left[\textcircled{S^R} \right]^{j_l} \right]^{\Delta_{L_l}} \end{array} \right]^{\Delta^{K(n)}}. \quad (3.16)$$

Whilst this expression looks complicated, it is in fact representing something very simple. To reveal this, let us define $c \equiv \sum_{i=1}^l L'_i + K$. Intuitively, this variable has the following meaning. Consider a diagram of some topology (with no effective propagators starting and ending on the same vertex). Now imagine cutting some number of the effective propagators. The variable c tells us how many cuts we have made; equation (3.16) represents the parent diagram, multiplied by the sum of all possible ways of cutting the parent diagram, such that c cuts is weighted with a factor of $(-1)^c$. Indeed, equation (3.16) reduces to:

$$\Upsilon_{s_0, j_0} \sum_{c=0}^L (-1)^c {}^L C_c \left[\left[\textcircled{S^R} \right]^{j_0} \right]^{\Delta^{s_0(n)}} \delta(s_0 - L) = S^{\text{R}(n)}. \quad (3.17)$$

(The sum over c forces $L = 0$, which in turn forces $s_0 = 0$; $j_0 = 1$ then follows by connectedness.) This completes the proof of (3.8).

We are now in a position to deduce a special case of (2.14). Returning to (3.8), let us set $\Lambda = \Lambda_0$. On the left-hand side, we now have the bare vertices. On the right-hand side, the $\overline{S}^{\text{R}(n)}$ are unaffected, being as they are independent of Λ , but we must remember to set $\Lambda = \Lambda_0$ in the $\overline{\Delta}$. Now, by construction we have:

$$\Lambda_0 \frac{\partial}{\partial \Lambda_0} \Big|_{\{P_{\Lambda_0}\}} S_{\Lambda=\Lambda_0}^{\text{R}(n)} = 0, \quad \forall n. \quad (3.18)$$

Comparing (3.18) and (3.8)—with $\Lambda = \Lambda_0$ —to (3.3) and (3.5), we deduce that the action constructed from the vertices $\overline{S}^{\text{R}(n)}$ must satisfy the following equation:

$$\frac{\partial}{\partial \Lambda_0} \Big|_{\varphi, \{P_{\Lambda_0}\}} \overline{S}^{\text{R}}[\varphi] = \frac{1}{2} \frac{\delta \overline{S}^{\text{R}}}{\delta \varphi} \cdot \frac{\partial \overline{\Delta}_{\Lambda_0}}{\partial \Lambda_0} \Big|_{\{P_{\Lambda_0}\}} \cdot \frac{\delta \overline{S}^{\text{R}}}{\delta \varphi} - \frac{1}{2} \frac{\delta}{\delta \varphi} \cdot \frac{\partial \overline{\Delta}_{\Lambda_0}}{\partial \Lambda_0} \Big|_{\{P_{\Lambda_0}\}} \cdot \frac{\delta \overline{S}^{\text{R}}}{\delta \varphi}. \quad (3.19)$$

This is clearly exactly equivalent to (2.14) with $\Lambda = 0$ [recall (3.9)]. Note that, at this stage, it would seem that we can (though need not) relax the condition that the propagator be massive. Whether or not we can use diagrammatic techniques to deduce (2.14) for any value of Λ , we leave as an open question. Our aim now is to interpret the $\overline{S}^{\text{R}(n)}$ for flow equations which, whilst perfectly valid ERG equations, cannot be derived from the Polchinski by simply rescaling the field. Note that, for such

equations the $\bar{S}^{\text{R}(n)}$ are no longer independent of Λ and so (3.19) could be rewritten to emphasise this fact:

$$\left. \frac{\partial}{\partial \Lambda_0} \right|_{\varphi, \{P_{\Lambda_0}\}} \bar{S}_{\Lambda=\Lambda_0}^{\text{R}}[\varphi] = \frac{1}{2} \frac{\delta \bar{S}_{\Lambda=\Lambda_0}^{\text{R}}}{\delta \varphi} \cdot \left. \frac{\partial \bar{\Delta}_{\Lambda_0}}{\partial \Lambda_0} \right|_{\{P_{\Lambda_0}\}} \cdot \frac{\delta \bar{S}_{\Lambda=\Lambda_0}^{\text{R}}}{\delta \varphi} - \frac{1}{2} \frac{\delta}{\delta \varphi} \cdot \left. \frac{\partial \bar{\Delta}_{\Lambda_0}}{\partial \Lambda_0} \right|_{\{P_{\Lambda_0}\}} \cdot \frac{\delta \bar{S}_{\Lambda=\Lambda_0}^{\text{R}}}{\delta \varphi}. \quad (3.20)$$

4. General ERGs

The Polchinski equation is but one of an infinite number of unrelated ERGs, all of which encode the same physics. The formulation of general ERGs follows simply from demanding that the partition function is invariant under the flow [20, 21]:

$$-\Lambda \partial_{\Lambda} e^{-S_{\Lambda}[\varphi]} = \int_x \frac{\delta}{\delta \varphi(x)} \left(\Psi_x[\varphi] e^{-S_{\Lambda}[\varphi]} \right), \quad (4.1)$$

where the Λ derivative is, as usual, performed at constant φ . The total derivative on the right-hand side ensures that the partition function $Z = \int \mathcal{D}\varphi e^{-S_{\Lambda}}$ is invariant under the flow.

The functional Ψ parametrizes (the continuum version of) a general Kadanoff blocking [22] in the continuum. To generate the family of flow equations to which the Polchinski equation belongs, we take:

$$\Psi_x = \frac{1}{2} \dot{\Delta}(x, y) \frac{\delta \Sigma_{\Lambda}}{\delta \varphi(y)}, \quad (4.2)$$

where we define $\dot{X} \equiv -\Lambda dX/d\Lambda$. At first sight, equation (4.2) seems to correspond to precisely the Polchinski equation. However, there are two potential differences. First, we need not identify the kernel, $\dot{\Delta}$, with $\dot{\Delta}_{\text{UV}}$ (it could differ e.g. by a multiplicative factor). Secondly, whilst we still take Σ to be given by (2.11), we can in principle allow \hat{S}_{Λ} to become a completely general action, the ‘seed action’ [8, 9, 10, 11], rather than just possessing a kinetic term. The only restrictions on the seed action are that it is infinitely differentiable and leads to convergent loop integrals [8].

Now, to find how S_{Λ} varies with Λ_0 , at constant $\{P_{\Lambda_0}\}$, we could integrate up (4.1) with respect to Λ and differentiate with respect to Λ_0 , but this does not seem to be particularly illuminating; rather, we will investigate the flow equations defined by (4.1) through their diagrammatic interpretation.

Instead of working with the flow equation produced by (4.1), directly, we will rescale the field according to $\varphi \rightarrow \sqrt{Z}\varphi$, where Z is the field strength renormalization. A particularly useful generalization of the Polchinski equation corresponds to shifting also $\Delta \rightarrow Z\Delta$ in (4.2). By doing this, the explicit powers of Z introduced on the right-hand side of the flow equation can be absorbed and so the flow equation reads:

$$-\Lambda \partial_{\Lambda} S_{\Lambda}[\varphi] + \frac{\gamma}{2} \varphi \cdot \frac{\partial S_{\Lambda}}{\partial \varphi} = \frac{1}{2} \frac{\delta S_{\Lambda}}{\delta \varphi} \cdot \dot{\Delta} \cdot \frac{\delta \Sigma_{\Lambda}}{\delta \varphi} - \frac{1}{2} \frac{\delta}{\delta \varphi} \cdot \dot{\Delta} \cdot \frac{\delta \Sigma_{\Lambda}}{\delta \varphi}, \quad (4.3)$$

where $\gamma \equiv \Lambda \partial_{\Lambda} \ln Z$ is the anomalous dimensions. Note that if we were now to identify Δ with Δ_{UV} then, modulo the general seed action buried in Σ_{Λ} , equation (4.3) looks like a version of the Polchinski equation where Z has been scaled out on the left-hand

side, but not on the right-hand side [9, 23, 24]; such a flow equation is a cousin and not a direct descendent of the Polchinski equation.

The diagrammatic form of the flow equation for the n -point vertex coefficient functions (i.e. symmetry factors and fields have been stripped off, as before) is given in figure 4, where we have again dropped the subscript Λ on the various actions.

$$\left(-\Lambda \frac{d}{d\Lambda} + \frac{1}{2}\gamma_n\right) \left[\textcircled{S} \right]^{(n)} = \frac{1}{2} \left[\begin{array}{c} \textcircled{\Sigma} \\ \bullet \\ \textcircled{S} \end{array} - \textcircled{\Sigma}^{\bullet} \right]^{(n)}$$

Figure 4. The diagrammatic form of the flow equation for vertices of the Wilsonian effective action.

From the diagrammatic form of the flow equation, a very powerful diagrammatic calculus has been developed [8] refined [10, 11, 15, 18, 19, 25, 26] and completed in [14], where it was finally understood how to apply it nonperturbatively in QCD. The key ingredient is the effective propagator relationship [8, 10, 14, 27]. The nonperturbative statement of this relationship is simply that the integrated ERG kernel, a.k.a. the effective propagator, Δ , has an inverse. Diagrammatically, we write this simply as

$$-\textcircled{\Delta^{-1}} = 1. \quad (4.4)$$

The reason that the effective propagator relationship is so useful is because it allows diagrams to be simplified: in any term where a Δ^{-1} is present and is attached to an effective propagator, we can collapse the structure down to the identity. In a typical calculation, the resulting diagrams cancel against terms generated elsewhere (see [8, 15, 18, 19, 26, 28] for examples).

Given that we have introduced Δ^{-1} vertex by hand, where is it that it appears in diagrams generated by the flow equation? The answer is that we simply pull them out of Wilsonian effective action vertices, defining reduced vertices, $S^{\text{R}(n)}$, as in (3.1) and (3.2a,3.2b), such that

$$\left[\textcircled{S^{\text{R}}} \right]^{(n)} \equiv \left[\textcircled{S} - \textcircled{\Delta^{-1}} \delta_{n,2} \right]^{(n)}, \quad (4.5)$$

and similarly for the seed action:

$$\left[\textcircled{\hat{S}^{\text{R}}} \right]^{(n)} \equiv \left[\textcircled{\hat{S}} - \textcircled{\Delta^{-1}} \delta_{n,2} \right]^{(n)}. \quad (4.6)$$

As before, reduction affects only the two-point vertex. Recall that in the case where we make the natural identification of Δ with the Δ_{UV} , it is clear that we can identify the reduced Wilsonian effective action vertices as the vertices of S_{Λ}^{int} . After the aforementioned cancellations have gone through, we end up with diagrams built from reduced vertices.

Now, just as before, we can introduce the $\bar{S}^{R(n)}$ according to (3.3), we can invert this expression according to (3.8) and we have (3.18). Consequently, we once again deduce the flow equation (3.20). However, this is not the end of the matter: for the flow equation (4.3), (3.5) is no longer true and so we must understand what the $\bar{S}_{\Lambda=\Lambda_0}^{R(n)}$ now represent.

To this end, we apply the new flow equation, shown in figure 4, to (3.3). Applying the diagrammatic calculus, as described in [14, 15, 18, 19], we derive the following (the details are presented in Appendix A):

$$\Lambda \frac{d}{d\Lambda} \bar{S}^{R(n)} + \frac{n\gamma}{2} \bar{S}^{R(n)} = \gamma \left[\left(\Delta^{-1} \right) \delta_{n,2} \right]^{(n)} - \sum_{s=0}^{\infty} \sum_{j=1}^{s+1} \Upsilon_{s,j-1} \left[\begin{array}{c} \hat{S}^R \\ \bullet \\ \left[\Delta^{-1} \right]^{(1)} \\ \left[S^R \right]^{j-1} \end{array} \right]^{\Delta^s(n)}. \quad (4.7)$$

We understand that the Δ^{-1} vertex in the final term must be decorated by any one of the n external fields.

The structure of the final term on the right-hand side has an intuitive explanation. We stated earlier that the reason the effective propagator relationship is so useful is because, in a typical calculation, any diagram in which Δ^{-1} attaches to an effective propagator cancels against some other term. Consequently, the only term involving Δ^{-1} which survives is the one for which it does not attach to an effective propagator; therefore it must be decorated by an external field.

Considering flow equations with a completely general seed action, it is not obvious how to make progress. However, if we suppose that the seed action has no interaction terms and, moreover, is given precisely by Δ^{-1} , then the right-hand side of (4.7) vanishes since \hat{S}^R is zero in this case [see (4.6)]. Given this restriction, equation (4.7) becomes:

$$\Lambda \frac{d}{d\Lambda} \left[Z \bar{S}^{R(2)}(k) \right] = \Lambda \frac{dZ}{d\Lambda} \Delta^{-1}(k), \quad (4.8)$$

$$\Lambda \frac{d}{d\Lambda} \left[Z^{n/2} \bar{S}^{R(n)}(k_i) \right] = 0, \quad n > 2. \quad (4.9)$$

This simplification will allow us to find a useful interpretation for the $\bar{S}_{\Lambda=\Lambda_0}^{R(n)}$.

What we would ideally like to do is relate the $\bar{S}_{\Lambda=\Lambda_0}^{R(n)}$ to the $\bar{S}_{\Lambda=0}^{R(n)}$, which encode the physics. However, there is a problem with this: we see from (4.8) that $\bar{S}^{R(2)}$ diverges in the $\Lambda \rightarrow 0$ limit [recall that $c^{-1}(k^2/\Lambda^2)$ diverges as $k^2/\Lambda^2 \rightarrow 0$]. By considering the flow equation (4.3), this can be traced back to the fact that $S^{R(2)}$ is no longer finite in this limit, either. It should be emphasised that this is not a sickness of the flow equation: even in the Polchinski case, the *full* Wilsonian effective action has divergences in the $\Lambda \rightarrow 0$ limit, brought about by the regularization of the kinetic term. However, in the Polchinski case, these divergences do not feed back into the $S^{\text{int}(n)}$, whereas in the more general case they do feed back into the $S^{R(2)}$. Now, even though the $\bar{S}^{R(n>2)}$ have

contributions involving $S^{R(2)}$ s, the $\bar{S}^{R(n>2)}$ are, themselves, finite in the limit $\Lambda \rightarrow 0$. This follows because each instance of $S^{R(2)}$ contributing to $\bar{S}^{R(n>2)}$ must be accompanied by an internal line, which ameliorates any divergences in the limit $\Lambda \rightarrow 0$. Indeed, it is straightforward to show from the flow equation for the two-point vertex that $S^{R(2)}$ can never diverge faster than Δ vanishes (see Appendix B).

Consequently, any 1PI contributions to $\bar{S}^{R(n>2)}$ possessing internal lines vanish because in there is always at least one more internal line than there are $S^{R(2)}$ vertices. However, one-particle reducible (1PR) diagrams can survive, if and only if they comprise a single $S^{R(n)}$ vertex attached to any number of $S^{R(2)}$ vertices. In other words, we have that

$$\lim_{\Lambda \rightarrow 0} \bar{S}^{R(n)}(k_1, \dots, k_n) = \lim_{\Lambda \rightarrow 0} \frac{S^{R(n)}(k_1, \dots, k_n)}{\prod_{i=1}^n [1 + S^{R(2)}(k_i)\Delta(k_i)]}, \quad n > 2, \quad (4.10)$$

where the right-hand side comes from summing the geometric series comprising strings of two-point vertices joined to the legs of the $S^{R(n)}$ vertex.

For $\bar{S}^{R(2)}$, the result is similar. Again, any 1PI diagrams (besides that comprising a single vertex) vanish in the limit $\Lambda \rightarrow 0$. Now consider the 1PR diagrams. If a 1PR diagram consists only of $S^{R(2)}$ vertices joined by internal lines then it diverges as $\Lambda \rightarrow 0$, since the number of divergent vertices is always one greater than the number of vanishing lines. However, suppose that the 1PR diagram possesses a (two-legged) 1PI sub-diagram. Then, putting this sub-diagram to one side for a moment, the rest of the diagram must be convergent in the $\Lambda \rightarrow 0$ limit since the number of $S^{R(2)}$ vertices is now equal to the number of internal lines as follows from the fact that each string of $S^{R(2)}$ s must be connected to the 1PI sub-diagram. However, the 1PI sub-diagram vanishes in the limit $\Lambda \rightarrow 0$ and so the diagram as a whole vanishes, also. This argument clearly works if we take further 1PI sub-diagrams and so we conclude that

$$\lim_{\Lambda \rightarrow 0} \bar{S}^{R(2)}(k) = \lim_{\Lambda \rightarrow 0} \frac{S^{R(2)}(k)}{1 + S^{R(2)}(k)\Delta(k)}. \quad (4.11)$$

Now, as before, let us set $Z_{\Lambda_0} = 1$, for simplicity. From (4.8) and (4.9) we have that

$$\bar{S}_{\Lambda_0}^{R(2)}(k) = Z_{\Lambda} \bar{S}_{\Lambda}^{R(2)}(k) + \int_{\Lambda}^{\Lambda_0} (d \ln \Lambda') \Lambda' \frac{dZ}{d\Lambda'} \Delta^{-1}(k), \quad (4.12)$$

$$\bar{S}_{\Lambda_0}^{R(n)}(k_i) = Z_{\Lambda}^{n/2} \bar{S}_{\Lambda}^{R(n)}(k_i). \quad (4.13)$$

The left-hand sides of (4.12) and (4.13) are finite, irrespective of Λ , and so, in (4.12) (in particular), we can safely take the limit $\Lambda \rightarrow 0$, since the divergence of the second term on the right-hand side must cancel the divergences of the first term. Thus, for the case where the Wilsonian effective action satisfies the flow equation (4.3), equation (3.20) tells us how finite combinations of the vertices of the low energy Wilsonian effective action evolve with Λ_0 , the bare interactions having been kept fixed.

5. Conclusion

We have investigated how the effective action of scalar field theory in D dimensions evolves as the bare scale at which we initiate a nonrenormalizable trajectory is changed, whilst keeping the bare interactions fixed. The simplest case is when the effective action satisfies the Polchinski equation; then we proved, directly from the path integral, that the variation of the effective action (at any scale) with the bare scale is given by an equation, (2.14), of the same form as the Polchinski equation but with a kernel of the opposite sign (and evaluated at the bare, rather than effective scale).

Following this, in preparation for the treatment of generalizations of the Polchinski equation, we showed that in the case where we focus on the low energy effective action, we could deduce (2.14) for $\Lambda = 0$ using diagrammatic techniques. The key to this was first to introduce the dressed vertices, $\bar{S}^{R(n)}$, according to (3.3), and then to show that the relationship between the $\bar{S}^{R(n)}$ and the $S^{R(m)}$ out of which they are built can be inverted, as in (3.8). The similarity between (3.3) and (3.8) is striking and merits further investigation. It should be emphasised that this result is true irrespective of the form of the flow equation. What the flow equation determines is the precise interpretation of the $\bar{S}^{R(n)}$. If the effective action satisfies the Polchinski equation, then the $\bar{S}^{R(n)}$ are independent of scale. Since they can be shown to reduce to the low energy effective action vertices for $\Lambda = 0$, it is clear that the $\bar{S}^{R(n)}$ must be equal to the $S_{\Lambda=0}^{R(n)}$.

Putting the interpretation of the $\bar{S}^{R(n)}$ to one side, we then focussed on the fact that they are invariants of the Polchinski equation and are built out of the $S^{R(m)}$. But, if we keep the bare parameters fixed, then by definition the $S_{\Lambda=\Lambda_0}^{R(n)}$ are invariants with respect to Λ_0 . Since the $S^{R(n)}$ are built out of the $\bar{S}^{R(m)}$ in the same way as the $\bar{S}^{R(n)}$ are built out of the $S^{R(m)}$, modulo the sign of the internal lines, this implies that the invariants with respect to Λ_0 , the $S_{\Lambda=\Lambda_0}^{R(n)}$, must follow from a Polchinski-like equation. In this way, we are able to diagrammatically deduce (3.20), which is true, whatever the flow equation satisfied by the effective action vertices.

Since (3.20) is written in terms of the $\bar{S}_{\Lambda=\Lambda_0}^{R(n)}$, the next task was to interpret these objects. If the effective action satisfies the Polchinski equation, this is easy. As mentioned already, in this case the $\bar{S}^{R(n)}$ are independent of Λ . Since it can be shown that they are given by the low energy effective action vertices for $\Lambda = 0$, it is clear that they must just be equal to $S_{\Lambda=0}^{R(n)}$. Consequently, (3.20) is equivalent to the special, but most interesting case of (2.14), namely $\Lambda = 0$.

For the case where the effective action satisfies generalizations of the Polchinski equation, matters are less clear. We predominantly focussed on a flow equation which is written in terms of the renormalized field but where the right-hand side does not follow from rescaling the field in the Polchinski equation. This flow equation, like the Polchinski equation, still has the simplest allowed seed action (blocking functional) and, as a consequence of this, the invariants take a simple form, given by (4.9). This allowed us to express the $\bar{S}_{\Lambda=\Lambda_0}^{R(n)}$ in terms of finite combinations of the vertices of the low

energy Wilsonian effective action. In the case of more general blocking functionals, the corresponding flow equation no longer admits invariants of a form where it is straightforward to relate the $\bar{S}_{\Lambda=\Lambda_0}^{R(n)}$ to the physical, low energy effective action vertices.

Appendix A. Flow of the $\bar{S}^{R(n)}$

In this appendix, we derive (4.7) by applying the diagrammatic form of the generalized flow equation, shown in figure 4 to (3.3). The first thing we require is the flow of a reduced vertex, which we deduce by substituting (4.5) into figure 4. For brevity, we henceforth drop the Kronecker- δ associated with (4.5), taking its presence to be implicit in the vertex with argument Δ^{-1} . Separating out all occurrences of Δ^{-1} we have:

$$\Lambda \frac{d}{d\Lambda} \left[\textcircled{S^R} \right]^{(n)} = \frac{1}{2} \left[n\gamma \left(\textcircled{S^R} + \textcircled{\Delta^{-1}} \right) - \begin{array}{c} \textcircled{S^R} \\ \bullet \\ \textcircled{\Sigma^R} \end{array} + 2 \begin{array}{c} \textcircled{\hat{S}^R} \\ \bullet \\ \textcircled{\Delta^{-1}} \end{array} + \begin{array}{c} \textcircled{\bullet} \\ \textcircled{\Sigma^R} \end{array} - \begin{array}{c} \textcircled{\bullet} \\ \textcircled{\Delta^{-1}} \end{array} \right]^{(n)} \quad (\text{A.1})$$

The final term can be discarded since it is a vacuum energy term, only contributing for $n = 0$ (this follows because the vertex Δ^{-1} must have precisely two legs).

Applying (A.1), we find that the flow of $\bar{S}^{R(n)}$ [see (3.3)] is as shown in figure A1.

There are a number of comments to make. In diagram D.1 the topmost vertex is decorated by *any* f legs; these can correspond to external legs or the ends of internal lines. The number of such decorations is $\#_f$. In diagram D.5 we could, for $j > 1$, reduced the upper limit on the sum over j by one, as follows from demanding that all diagrams are connected. Finally, we have noticed from (3.4) that $2s\Upsilon_{s,j} = \Upsilon_{s-1,j}$ and $j\Upsilon_{s,j} = -\Upsilon_{s,j-1}$.

The strategy now is to process diagrams containing a Δ^{-1} . Let us start with diagram D.4. We can decorate the Δ^{-1} in two ways: either with an external field, after which we can do nothing further—this yields the final term in (4.7)—, or with an end of an internal line. But, in the latter case, we can apply the effective propagator relationship (4.4). The resulting terms exactly cancel the seed action contributions to diagrams D.3 and D.5. What of the surviving, contributions to these two diagrams, which comprise only Wilsonian effective action vertices? These are exactly cancelled by diagram D.6. In summary, then, the final four diagrams of figure A1 combine to give:

$$\text{D.3} + \text{D.4} + \text{D.5} + \text{D.6} = - \sum_{s=0}^{\infty} \sum_{j=1}^{s+1} \Upsilon_{s,j-1} \left[\begin{array}{c} \textcircled{\hat{S}^R} \\ \bullet \\ \left[\textcircled{\Delta^{-1}} \right]^{(1)} \\ \left[\textcircled{S^R} \right]^{j-1} \end{array} \right]^{\Delta^s(n)}, \quad (\text{A.2})$$

$$\begin{aligned}
\Lambda \frac{d}{d\Lambda} \bar{S}^{R(n)} &= -\frac{1}{2} \sum_{s=0}^{\infty} \sum_{j=1}^{s+1} \Upsilon_{s,j-1} \left[\begin{array}{c} \text{D.1} \\ \text{D.2} \end{array} \right]^{(f)} \Delta^{s(n)} \\
&\quad + \frac{1}{2} \sum_{s=0}^{\infty} \sum_{j=1}^{s+1} \Upsilon_{s,j-1} \left[\begin{array}{c} \text{D.3} \quad \text{D.4} \quad \text{D.5} \\ \text{D.6} \end{array} \right] \Delta^{s(n)} \\
&\quad - \frac{1}{2} \sum_{s=1}^{\infty} \sum_{j=1}^{s+1} \Upsilon_{s-1,j} \left[\begin{array}{c} \text{D.6} \end{array} \right] \Delta^{s-1(n)}
\end{aligned}$$

Figure A1. The flow of $\bar{S}^{R(n)}$, as generated by the flow equation of figure 4.

where we recall that the notation demands that the Δ^{-1} is decorated by one of the external fields.

Next, let us examine diagram D.2. There are three (useful) ways we can decorate the Δ^{-1} . If $s = 0$ and $n = 2$, we can decorate it with the two external fields. Otherwise, we can decorate it with any one of the n external fields and one end of an internal line, or with two ends of two different internal lines (if we decorate it with the ends of one internal line, then we end up with a vacuum energy contribution). We therefore find the following:

$$\text{D.2} = -\gamma \Upsilon_{0,0} \left[\Delta^{-1} \right]^{(n)} - n\gamma \bar{S}^{R(n)} - \frac{\gamma}{2} \sum_{s=2}^{\infty} \sum_{j=2}^{s+1} \Upsilon_{s-2,j-1} \left[\begin{array}{c} \text{D.7} \\ \Delta \\ \text{D.6} \end{array} \right] \Delta^{s-2(n)}.$$

Notice that the final diagram comes from attaching two effective propagators to the Δ^{-1} , whereupon one of them is removed via the effective propagator relationship (4.4). The one which remains appears as the Δ above the vertex; we will call this effective propagator special. Now, consider creating some fully fleshed out diagram from D.7 [19]. The total of $s + 1$ effective propagators are to be divided into q sets, each containing L_i effective propagators. Since the special effective propagator can reside in any of

these sets, there are q different ways to make the sets. The overall combinatoric factor associated with this partitioning is, therefore,

$$\frac{(s-2)!}{\prod_i L_i!} \sum_i L_i = \frac{(s-1)!}{\prod_i L_i!},$$

which is just the combinatoric factor expected from partitioning $s-1$ effective propagators into q sets. Therefore, we can combine the special effective propagator with the rest (to give Δ^{s-1}) but, counterintuitively, the combinatoric factor of the diagram, $\Upsilon_{s-2,j-1}$, *stays the same!* For convenience, we now shift $s \rightarrow s+1$, $j \rightarrow j+1$ and so obtain:

$$\text{D.7} = -\frac{\gamma}{2} \sum_{s=1}^{\infty} \sum_{j=1}^{s+1} \Upsilon_{s-1,j} \left[\left[\textcircled{S^R} \right]^j \right]^{\Delta^{s(n)}}$$

Finally, we process diagram D.1. The key here is to recognize that any of the j vertices could be the one with the f decorations, and that f is summed over. Now, the total number of internal plus external legs is $2s+n$. Therefore, we can replace $\#_f$ with $(2s+n)/j$, yielding:

$$\text{D.1} = \frac{n\gamma}{2} \overline{S}^{\text{R}(n)} + \frac{\gamma}{2} \sum_{s=1}^{\infty} \sum_{j=1}^{s+1} \Upsilon_{s-1,j} \left[\left[\textcircled{S^R} \right]^j \right]^{\Delta^{s(n)}}$$

Putting everything together, we have:

$$\text{D.1} + \text{D.2} = \gamma \left[\left[\textcircled{\Delta^{-1}} \right]^{(n)} - \frac{n\gamma}{2} \overline{S}^{\text{R}(n)} \right] \quad (\text{A.3})$$

Summing up (A.2) and (A.3) we reproduce (4.7), as desired.

Appendix B. Divergence of the Two-Point Vertex

In this appendix we will show that, in the limit $\Lambda \rightarrow 0$, the reduced two-point vertex cannot diverge faster than Δ^{-1} . To this end, consider keeping only those two-point contributions from (A.1) which diverge, in this limit:

$$\Lambda \frac{d}{d\Lambda} S^{\text{R}(2)}(p) \sim \gamma [S^{\text{R}(2)}(p) + \Delta^{-1}(p)] - S^{\text{R}(2)}(p) \dot{\Delta}(p) S^{\text{R}(2)}(-p). \quad (\text{B.1})$$

Let us now suppose that $S^{\text{R}(2)}(p)$ diverges faster than Δ^{-1} , as $\Lambda \rightarrow 0$. But, $\dot{\Delta}$ does not vanish faster than Δ , in this limit. Indeed, if $C_{\text{UV}} \sim (p^2/\Lambda^2)^{-r}$ for large p^2/Λ^2 , then $\dot{\Delta}$ and Δ vanish at the same rate; if, instead, $C_{\text{UV}} \sim \exp(-p^2/\Lambda^2)$, then $\dot{\Delta}$ vanishes more slowly than Δ . Consequently, for $\Lambda \rightarrow 0$, and given our initial assumption, it is clear that the final term on the right-hand side of (B.1) is the leading term (so long as γ does not diverge). But, if

$$\Lambda \frac{d}{d\Lambda} S^{\text{R}(2)}(p) \sim -S^{\text{R}(2)}(p) \dot{\Delta}(p) S^{\text{R}(2)}(-p),$$

then

$$S^{\text{R}(2)}(p) \sim -\Delta^{-1}(p),$$

violating the original assumption that $S^{\text{R}(2)}(p)$ diverges faster than Δ^{-1} as $\Lambda \rightarrow 0$.

Acknowledgments

It is a pleasure to thank Clifford Johnson for his kind hospitality at USC, where important parts of this work were done, and Franics Dolan, Denjoe O'Connor, Joe Polchinski and Hugh Osborn for useful discussions.

Bibliography

- [1] K. Wilson and J. Kogut, “The Renormalization group and the epsilon expansion,” *Phys. Rept.* **12** (1974) 75.
- [2] F. J. Wegner and A. Houghton, “Renormalization group equation for critical phenomena,” *Phys. Rev. A* **8** (1973) 401.
- [3] J. Polchinski, “Renormalization And Effective Lagrangians,” *Nucl. Phys. B* **231** (1984) 269.
- [4] T. R. Morris, “Elements of the continuous renormalization group,” *Prog. Theor. Phys.* **131** (1998) 395, [hep-th/9802039](#).
- [5] P. Hasenfratz and F. Niedermayer, “Perfect Lattice Action For Asymptotically Free Theories,” *Nucl. Phys. B* **414** (1994) 785, [hep-lat/9308004](#).
- [6] G. K. C. Kopper and M. Salmhofer, “Perturbative Renormalization And Effective Lagrangians In Φ^4 In Four-Dimensions,” *Helv. Phys. Acta* **65** (1992) 32.
- [7] M. Beneke, “Renormalons,” *Phys. Rept.* **317** (1999) 1, [hep-th/9807443](#).
- [8] S. Arnone, A. Gatti, and T. R. Morris, “A proposal for a manifestly gauge invariant and universal calculus in Yang-Mills theory,” *Phys. Rev. D* **67** (2003) 085004, [hep-th/0209162](#).
- [9] S. Arnone, A. Gatti, T. R. Morris, and O. J. Rosten, “Exact scheme independence at two loops,” *Phys. Rev. D* **69** (2004) 065009, [hep-th/0309242](#).
- [10] S. Arnone, T. R. Morris, and O. J. Rosten, “A Generalised manifestly gauge invariant exact renormalisation group for SU(N) Yang-Mills,” *Eur. Phys. J. C* **50** (2007) 467, [hep-th/0507154](#).
- [11] T. R. Morris and O. J. Rosten, “A manifestly gauge invariant, continuum calculation of the SU(N) Yang-Mills two-loop beta function,” *Phys. Rev. D* **73** (2006) 065003, [hep-th/0508026](#).
- [12] P. Hasenfratz and J. Nager, “The Cutoff Dependence of the Higgs Meson Mass and the Onset of New Physics in the Standard Model,” *Z. Phys.* **37** (1988) 477.
- [13] T. R. Morris, “The Exact renormalization group and approximate solutions,” *Int. J. Mod. Phys. A* **9** (1994) 2411, [hep-ph/9308265](#).
- [14] O. J. Rosten, “Universality from very general nonperturbative flow equations in QCD,” *Phys. Lett. B* **645** (466) 2007, [hep-th/0611323](#).
- [15] O. J. Rosten, “A primer for manifestly gauge invariant computations in SU(N) Yang-Mills,” *J. Phys. A* **39** (2006) 8699, [hep-th/0507166](#).
- [16] T. R. Morris, “On truncations of the exact renormalization group,” *Phys. Lett. B* **334** (1994) 355, [hep-th/9405190](#).
- [17] K. I. Aoki, K. Morikawa, W. Souma, J. I. Sumi, and H. Terao, “Rapidly converging truncation scheme of the exact renormalization group,” *Prog. Theor. Phys.* **99** (1998) 451, [hep-th/9803056](#).
- [18] O. J. Rosten, “Scheme independence to all loops,” *J. Phys. A* **39** (2006) 8699, [hep-th/0507166](#).
- [19] O. J. Rosten, “A manifestly gauge invariant and universal calculus for SU(N) Yang-Mills,” *Int. J. Mod. Phys. A* **21** (2006) 4627, [hep-th/0602229](#).
- [20] F. J. Wegner, “Some Invariance Properties of the Renormalization Group,” *J. Phys. C* **7** (1974) 2098.
- [21] T. R. Morris and J. L. Latorre, “Exact scheme independence,” *JHEP* **0011** (2000) 004, [hep-th/0008123](#).
- [22] L. P. Kadanoff, “Scaling laws for Ising models near $T(c)$,” *Physics* **2** (1966) 263.

- [23] R. D. Ball, P. E. Haagensen, J. I. Latorre, and E. Moreno, “Scheme Independence And The Exact Renormalization Group,” *Phys. Lett. B* **347** (1995) 80, [hep-th/9411122](#).
- [24] S. Arnone, A. Gatti, and T. R. Morris, “Exact scheme independence at one loop,” *JHEP* **0205** (2002) 059, [hep-th/0201237](#).
- [25] O. J. Rosten, *The manifestly gauge invariant exact renormalisation group*. PhD thesis, Southampton U., 2005. [hep-th/0506162](#).
- [26] S. Arnone, T. R. Morris, and O. J. Rosten, “Manifestly gauge invariant QED,” *JHEP* **0510** (2005) 115, [hep-th/0505169](#).
- [27] T. R. Morris and O. J. Rosten, “Manifestly gauge invariant QCD,” *J. Phys. A* **39** (2006) 11657, [hep-th/0606189](#).
- [28] O. J. Rosten, “General computations without fixing the gauge,” *Phys. Rev. D* **74** (2006) 125006, [hep-th/0604183](#).